CHIN. PHYS. LETT. Vol. 32, No. 5 (2015) 058104

# Left-Handedness with Three Zero-Absorption Windows Tuned by the Incoherent Pumping Field and Inter-Dot Tunnelings in a GaAs/AlGaAs Triple Quantum Dots System *

ZHAO Shun-Cai(赵顺才)[1**], ZHANG Shuang-Ying(张双颖)[1], WU Qi-Xuan(吴奇宣)[2], JIA Jing(贾靖)[1]

[1]*Physics department, Kunming University of Science and Technology, Kunming 650500*
[2]*College of English, Kunming University of Science and Technology, Kunming 650500*

(Received 13 December 2014)

*Left-handedness with three zero-absorption windows is achieved in a triple-quantum-dot system. With the typical parameters of a GaAs/AlGaAs heterostructure, the simultaneous negative relative electric permittivity and magnetic permeability are obtained by the adjustable incoherent pumping field and two inter-dot tunnelings. Furthermore, three zero-absorption windows in the left-handedness frequency bands are observed. The left-handedness with zero-absorption in the solid state heterostructure may solve the challenges not only in the left-handed materials achieved by the photonic resonant scheme but also in the application of negative refractive materials with a large amount of absorption.*

*PACS: 81.07.Ta, 03.67.Ac, 73.21.La, 78.67.Hc, 42.50.Gy* DOI: 10.1088/0256-307X/32/5/058104

Recently, many experimental and theoretical investigations have been devoted to understanding and constructing the micro-structured materials possessing exotic optical properties such as left-handedness.[1] In such a material characterized by negative electric and magnetic permittivity (left-handed materials, LHMs), many surprising phenomena occur, including amplification of evanescent waves,[2] sub-wavelength focusing,[3] reversals of both Snell's law and Doppler shift,[1] etc. Several approaches, such as artificial structures,[4–6] photonic crystals,[7,8] chiral materials[9–11] and photonic resonant media[12–14] gave birth to LHMs. However, the major challenge in the photonic resonant scheme is to have two levels separated at optical frequencies with a non-vanishing magnetic dipole matrix element.[8] Therefore, the solid state heterostructures with excitonic energy levels or quantum dots[15] with a suitable spectrum may be the candidate.

With the flaw of photonic resonant scheme in mind, the triple quantum dot (TQD) arrays fabricated by a GaAs/AlGaAs heterostructure[16] may be an ideal candidate due to the fact that the TQD possesses the atom vapors' features in solid-state structures and provides a fully tunable platform via the coherent coupling of quantum states. On account of its potential applications the TQD system has attracted intense investigations[17–25] including the charge and spin transport properties,[19] the manipulation of three-electron spin states,[20] spin-orbit effects,[21] a resonant exchange qubit[22] and spin blockade turning to bipolar.[23,24] The typical TQD grown by molecular epitaxy on a [001] GaAs substrate has the typical heights span of 1.5–2.5 nanometer via the InAs imbedded into the GaAs/$Al_{0.45}Ga_{0.55}As$ layer,[25] and their volumes can be modeled as three spheres with 3.5 nm in height and 35 nm in diameter for QD1, 2.5 nm in height and 25 nm in diameter for QD2 and QD3,[26] as shown in Fig. 1(a).

In this Letter, we theoretically investigate the left-handedness and absorption property of this TQD. It is found that Left-handedness with three zero-absorption windows tuned by the incoherent pumping field and two inter-dot tunnelings of this TQD is achieved, as can overcome the defect in the photonic resonant scheme and the limitation in the application of negative refractive materials with a large amount of absorption.

The cross section of the TQD nanostructure under consideration is shown in Fig. 1(a), and its corresponding energy levels are depicted in Fig. 1(b). The energy levels of the TQD molecule consist of three dots, which are coupled by the electron tunneling and form four atomic levels. Levels $|1\rangle$ and $|2\rangle$ are the lower and upper conducting band levels of QD1, respectively. Levels $|3\rangle$ and $|4\rangle$ are the excited conducting levels of QD2 and QD3, respectively. The energy differences of the three excited conducting levels from the lower level are assumed to be large, thus their corresponding tunneling couplings are ignored. However, the tunnel barrier can be manipulated by the positioned gate electrode between the neighboring QDs.[27] Thus levels $|3\rangle$ and $|4\rangle$ can become closer to level $|2\rangle$ via the gate voltage. An incoherent pump field with pumping rate denoted by $\Gamma$ and a weak probe field with Rabi frequency $\Omega_{\rm p}$ and frequency $\omega_{\rm p}$ are coupling the transitions $|1\rangle$ and $|2\rangle$. The electric and magnetic components (corresponding to Rabi frequency $\Omega_{\rm e} = \rho_{21}E_{\rm p}/\hbar$ and $\Omega_{\rm b} = m_{31}B_{\rm p}/\hbar$) of the probe field interact with the transitions $|1\rangle$ and $|2\rangle$ as well as $|1\rangle$ and $|3\rangle$, respectively. Under the coupling of the probe field with the QD1, the electron can be excited from the band $|1\rangle$ to

*Supported by the National Natural Science Foundation of China under Grant No 61205205, and the Foundation for Personnel Training Projects of Yunnan Province under Grant No KKSY201207068.
**Corresponding author. Email: zscnum1@126.com; zscgroup@kmust.edu.cn
© 2015 Chinese Physical Society and IOP Publishing Ltd

$|2\rangle$, then be transferred to QD2 and QD3 (the levels $|3\rangle$ and $|4\rangle$) via the tunneling $T_{\rm a}$ and $T_{\rm b}$. $T_{\rm a}$ and $T_{\rm b}$ are the electron tunneling matrix elements between the triple QDs. The probability of electron tunneling from the first QD1 in state $\Psi$ with energy $E_\Psi$ to the second QD2 in state $\Phi$ with energy $E_\Phi$ can be described by Fermi's golden rule[28] $p = \frac{2\pi}{\hbar}|T_{\rm e}|^2\delta(E_\Psi - E_\Phi)$. Thus the tunneling matrix element in the barrier region between the QDs can be integrated over a surface

$$T_{\rm e} = \frac{\hbar}{2m}\int_{z=z_0}\Big(\Phi^*\frac{\partial\Psi}{\partial z} - \Psi^*\frac{\partial\Phi^*}{\partial z}\Big)ds, \qquad (1)$$

where $m$ is the electron's effective mass, and $z_0$ is in the barrier. The tunneling matrix element $T_{\rm e}$ can be tuned by modifying the bias[29] applied to the QDs molecule due to the relation

$$I = \frac{4e\pi}{\hbar}\int_0^{eV}\varrho_1(E_{\rm F} - eV + \varepsilon)\varrho_2(E_{\rm F} + \varepsilon)|T_{\rm e}|^2 d\varepsilon, \quad (2)$$

where $I$ is the current which is proportional to the local state density of each QD ($\varrho_1$, $\varrho_2$) with the Fermi energy ($E_{\rm F}$). Under the rotating wave approximation, we write the total Hamiltonian describing the interaction of the probe and incoherent pumping fields with the TQD with neglect from the hole tunneling as follows:

$$\begin{aligned} H = \sum_{i=1}^{4} E_i|i\rangle\langle i| + [(&\Omega_{\rm e}e^{-i\omega_{\rm p}t}|1\rangle\langle 2| \\ &+ \Omega_{\rm b}e^{-i\omega_{\rm p}t}|1\rangle\langle 3| + \varepsilon D|1\rangle\langle 2| \\ &+ T_{\rm a}|2\rangle\langle 3| + T_{\rm b}|3\rangle\langle 4|) + {\rm H.c.}], \end{aligned} \qquad (3)$$

where $E_i = \hbar\omega_i$ is the energy of level $|i\rangle$, and $\varepsilon$ is the electrical amplitude of the incoherent pumping field with $D$ being the dipole moment corresponding to the transition from $|1\rangle$ to $|2\rangle$. By using the density-matrix approach, the time-evolution of the TQD system can be obtained as

$$\begin{aligned} \dot\rho_{11} =& (\gamma_{21} + \Gamma)\rho_{22} + \gamma_{31}\rho_{33} + \gamma_{41}\rho_{44} \\ &+ i(\Omega_{\rm e}\rho_{21} - \Omega_{\rm e}^*\rho_{12}) - \Gamma\rho_{11}, \\ \dot\rho_{22} =& -(\gamma_{21} + \Gamma)\rho_{22} - i(\Omega_{\rm e}\rho_{21} - \Omega_{\rm e}^*\rho_{12}) \\ &+ i(T_{\rm a}^*\rho_{32} - T_{\rm a}\rho_{23}) + \Gamma\rho_{11}, \\ \dot\rho_{33} =& -\gamma_{31}\rho_{33} + i(T_{\rm a}\rho_{23} - T_{\rm a}^*\rho_{32}) \\ &- i(T_{\rm b}\rho_{34} - T_{\rm b}^*\rho_{43}), \\ \dot\rho_{44} =& -\gamma_{41}\rho_{44} + i(T_{\rm b}\rho_{34} - T_{\rm b}^*\rho_{43}), \\ \dot\rho_{12} =& (i\Delta_{\rm p} - \Gamma_{21} - \Gamma)\rho_{12} \\ &- i\Omega_{\rm e}(\rho_{11} - \rho_{22}) - iT_{\rm a}\rho_{13}, \\ \dot\rho_{13} =& [i(\Delta_{\rm p} + \omega_{12}) - \Gamma_{31} - \Gamma/2]\rho_{13} \\ &+ i\Omega_{\rm b}\rho_{23} - i(T_{\rm a}^*\rho_{12} + T_{\rm b}\rho_{14}), \\ \dot\rho_{14} =& [i(\Delta_{\rm p} + \omega_{12} + \omega_{23}) - \Gamma_{41} - \Gamma/2]\rho_{14} \\ &+ i\Omega_{\rm e}\rho_{24} - iT_{\rm b}^*\rho_{13}, \\ \dot\rho_{32} =& -(i\omega_{23} + \Gamma_{12} + \Gamma/2)\rho_{32} - iT_{\rm a}(\rho_{33} - \rho_{22}) \\ &- i\Omega_{\rm b}\rho_{31} + iT_{\rm b}^*\rho_{42}, \\ \dot\rho_{42} =& -[i(\omega_{23} + \omega_{34}) + \Gamma_{42} + \Gamma/2]\rho_{42} \\ &- i(T_{\rm a}\rho_{43} - T_{\rm b}\rho_{32}) - i\Omega_{\rm e}\rho_{41}, \\ \dot\rho_{43} =& -(i\omega_{34} + \Gamma_{43})\rho_{43} \\ &- iT_{\rm b}(\rho_{44} - \rho_{33}) - iT_{\rm a}^*\rho_{42}, \\ 1 =& \rho_{11} + \rho_{22} + \rho_{33} + \rho_{44}, \end{aligned} \qquad (4)$$

where $\omega_{ij} = \omega_{i1} - \omega_{j1}$, $i, j = 2$, 3 and 4, and $\Delta_{\rm p} = \omega_{21} - \omega_{\rm p}$. The total decay rates of the TQD are added phenomenologically in the above density matrix Eq. (4), which include the spontaneous emission rates and dephasing rates. The spontaneous emission rates for sub-band $|i\rangle$ due to the longitudinal optical (LO) phonon emission events[30] are denoted by $\gamma_{i1}$. The total decay rates $\Gamma_{ij}$ ($i \neq j$) are given by $\Gamma_{i1} = \gamma_{i1}/2 + \gamma_{i1}^{\rm dph}$, $\Gamma_{ij} = (\gamma_{i1} + \gamma_{j1})/2 + \gamma_{ij}^{\rm dph}$, $i, j = 2$, 3 and 4, and $i \neq j$, in which $\gamma_{ij}^{\rm dph}$ is the dominant mechanism in a semiconductor solid-state system and determined by electron-electron, interface roughness and phonon scattering processes.

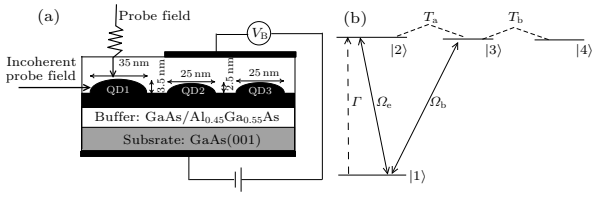


**Fig. 1.** (a) Cross section of the InAs TQD imbedded into a GaAs/$Al_{0.45}Ga_{0.55}$As layer with the probe and incoherent pumping fields. (b) The quantized energy levels for the TQD interacting with the probe and incoherent pumping fields. The electric and magnetic components of the probe field are coupled to the level pairs $|1\rangle$–$|2\rangle$ and $|1\rangle$–$|3\rangle$, respectively.

In the TQD molecule, the classical electric polarizability defined by its Fourier transform $\boldsymbol{p}_{\rm e}(\omega_{\rm p}) = \epsilon_0\alpha_{\rm e}(\omega_{\rm p})\boldsymbol{E}(\omega_{\rm p})$ is a rank 2 tensor and is related to the mean value of the atomic electric-dipole moment operators via the definition $\boldsymbol{P}_{\rm e} = {\rm Tr}\{\hat\rho\boldsymbol{d}\} = \rho_{12}d_{21} + {\rm c.c.}$, where Tr stands for trace. In the following, the polarizability at the frequency $\omega_{\rm P}$ of the incident probe field $\boldsymbol{E}_{\rm p}$ is considered, and we pay close attention to the $\omega_{\rm P}$-dependent $\alpha_{\rm e}(\omega_{\rm P}) \equiv \alpha_{\rm e}$. When $\boldsymbol{E}_{\rm p}$ is parallel to the atomic dipole $\boldsymbol{d}_{21}$, $\alpha_{\rm e}$ is a scalar and its expression is obtained to be

$$\alpha_{\rm e} = \frac{d_{21}\rho_{12}}{\epsilon_0 E_{\rm p}} = \frac{|\,d_{21}\,|^2\,\rho_{12}}{\epsilon_0\hbar\Omega_{\rm e}}. \qquad (5)$$

Similarly, the classical magnetic polarizations of the TQD molecule $\boldsymbol{P}_{\rm m}(\omega_{\rm P}) = \mu_0\alpha_{\rm m}\boldsymbol{E}(\omega_{\rm p})$, which is related to the mean value of the dipole moment operator through $\boldsymbol{P}_{\rm m} = {\rm Tr}\{\hat\rho\boldsymbol{\mu}\} = \rho_{31}\mu_{13} + {\rm c.c.}$ When the TQD molecule's magnetic dipole is perpendicular to the induced electric dipole, the magnetizability $\alpha_{\rm m}$ is a scalar via the classical Maxwell's electromagnetic wave-vector relation. Then $\alpha_{\rm m}$ is achieved as follows:

$$\alpha_{\rm m} = \frac{\mu_0\mu_{13}\rho_{31}}{B_{\rm p}} = \frac{\mu_0\,|\,\mu_{13}\,|^2\,\rho_{31}}{\hbar\Omega_{\rm b}}. \qquad (6)$$

According to the Clausius–Mossotti relations, the relative permittivity and relative permeability of the TQD system are expressed as[31,32]

$$\epsilon_r = \frac{1+\frac{2}{3}N\alpha_{\rm e}}{1-\frac{1}{3}N\alpha_{\rm e}}, \quad \mu_r = \frac{1+\frac{2}{3}N\gamma_{\rm m}}{1-\frac{1}{3}N\gamma_{\rm m}}. \tag{7}$$

Then the expressions for the electric permittivity and magnetic permeability of the TQD molecule are obtained. In the following, the left-handedness and absorption property in the TQD are discussed numerically by Eqs. (5)–(7) with the steady-state solution to Eq. (4). The simultaneously negative permittivity and permeability, negative refraction with triple zero-absorptive windows will be observed in this TQD system.

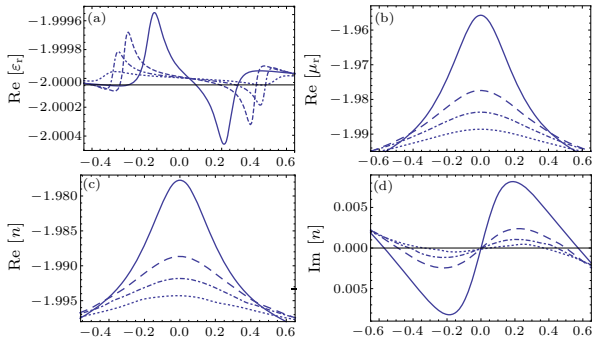


**Fig. 2.** (Color online) The values of Re[$\epsilon_r$], Re[$\mu_r$], Re[$n$], Im[$n$] versus the probe detuning $\frac{\Delta_{\rm p}}{\Gamma_{10}}$. Left-handedness tuned by the incoherent pumping field $\Gamma$: $\Gamma$=0 (dotted curves), $\Gamma = 0.2\Gamma_{10}$ (dash-dotted curves), $\Gamma = 0.3\Gamma_{10}$ (dashed curves), $\Gamma = 0.4\Gamma_{10}$ (solid curves), where $\Omega_{\rm p} = 0.05\Gamma_{10}$, $T_{\rm a} = 0.25\Gamma_{10}$, $T_{\rm b} = 0.60\Gamma_{10}$, $\omega_{12} = \omega_{23}$=0, $\Gamma_{10} = 1.6\gamma$ and $\gamma$=1 GHz.

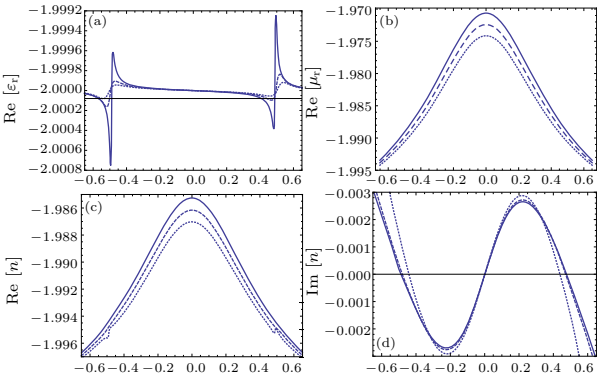


**Fig. 3.** (Color online) The values of Re[$\epsilon_r$], Re[$\mu_r$], Re[$n$], Im[$n$] versus the probe detuning $\frac{\Delta_{\rm p}}{\Gamma_{10}}$. Left-handedness tuned by the tunneling $T_{\rm a}$: $T_{\rm a} = 0.23\Gamma_{10}$ (dotted curves), $T_{\rm a} = 0.235\Gamma_{10}$ (dashed curves), $T_{\rm a} = 0.24\Gamma_{10}$ (solid curves), $\Gamma = 0.2\Gamma_{10}$, and the other parameters are the same as those in Fig. 2.

We investigate left-handedness and absorption property of the TQD via the numerical results. Several typical parameters of the GaAs/AlGaAs heterostructure are selected from the practical case: the sheet density of the TQD is taken as $3.7 \times 10^{11}\,{\rm cm}^{-2}$,[33] the electric transition dipole moment is chosen from the measured parameter: $d_{12} = 2.335 \times 1.602 \times 10^{-19}\,{\rm cm}$,[34] and the magnetic transition dipole moment is chosen from the typical parameter $\mu_{23} = 7.0 \times 10^{-23}\,{\rm cm}^2{\rm s}^{-1}$.[35] The other parameters are scaled by the typically slow dephasing rates $\Gamma_{10} = 1.6\gamma$, $\gamma = 1\,{\rm GHz}$,[36] $\Omega_{\rm p} = 0.05\Gamma_{10}$, and $\omega_{12} = \omega_{23} = 0$.

Figure 2 shows the calculated real parts of the relative electric permittivity Re[$\epsilon_r$], magnetic permeability Re[$\mu_r$] and relative refractive index $n$ of the TQD system versus the probe frequency detuning $\Delta_{\rm p}$, which are tuned by the incoherent pumping field. The absorption property of the TQD system can be described by the imaginary part of the relative refractive index Im[$n$]. The left-handedness with simultaneous negative Re[$\epsilon_r$], Re[$\mu_r$] and Re[$n$] is observed in Fig. 2. It should be noted that the increasing incoherent pumping field can enhance the negative response of the TQD system, which is shown by the dotted curves ($\Gamma = 0$), dash-dotted curves ($\Gamma = 0.2\Gamma_{10}$), dashed curves ($\Gamma = 0.3\Gamma_{10}$) and solid curves ($\Gamma = 0.4\Gamma_{10}$). This is the consequence of more electrons excited from $|1\rangle$ to $|2\rangle$ by the incoherent pumping field. However, the triple transparency windows shown by the imaginary part of relative refractive index Im[$n$] with two of them symmetrically distributing on both sides of the resonant position remain in the left-handed frequency band when the incoherent pumping field is tuned.

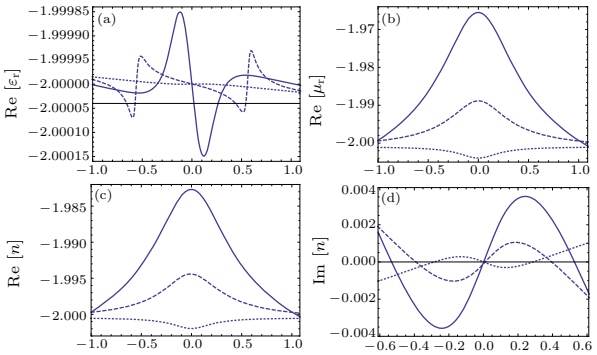


**Fig. 4.** (Color online) The values of Re[$\epsilon_r$], Re[$\mu_r$], Re[$n$], Im[$n$] versus the probe detuning $\frac{\Delta_{\rm p}}{\Gamma_{10}}$. Left-handedness tuned by the tunneling $T_{\rm b}$: $T_{\rm b} = 0.35\Gamma_{10}$ (dotted curves), $T_{\rm b} = 0.50\Gamma_{10}$ (dashed curves), $T_{\rm b} = 0.65\Gamma_{10}$ (solid curves), $T_{\rm a} = 0.24\Gamma_{10}$, and the other parameters are the same as those in Fig. 3.

To visualize the effect of inter-dot tunneling $T_{\rm a}$ and $T_{\rm b}$ on the left-handedness and absorption, Figs. 3 and 4 show the Re[$\epsilon_r$], Re[$\mu_r$], Re[$n$], Im[$n$] of the TQD system versus the inter-dot tunneling $T_{\rm a}$ and $T_{\rm b}$ while keeping the same incoherent pumping field. As is expected, the left-handed behavior is observed in Figs. 3 and 4. In Fig. 3 the pumping rate of the incoherent pumping field is set as $\Gamma = 0.2\Gamma_{10}$, and the tunneling $T_{\rm a}$ is set as $T_{\rm a} = 0.23\Gamma_{10}$ (dotted curves), $T_{\rm a} = 0.235\Gamma_{10}$ (dashed curves) and $T_{\rm a} = 0.24\Gamma_{10}$ (solid curves), which can be varied by the external gate voltage. The real parts of the electric permittivity Re[$\epsilon_r$], magnetic permeability Re[$\mu_r$] and relative refractive index Re[$n$] of the TQD system show the

gradual increasing negative response via the increasing tunneling $T_a$. In the curves of Im[$n$], there are three zero absorption windows, and two of them symmetrically distribute on both sides of the resonant dot when the tunneling $T_a$ is varied strongly.

As shown in Fig. 4, the TQD system shows left-handedness with the negative Re[$\epsilon_r$], Re[$\mu_r$] and relative refractive index Re[$n$] when the tunneling $T_b$ is varied by $T_b = 0.35\Gamma_{10}$ (dotted curves), $T_b = 0.50\Gamma_{10}$ (dashed curves), $T_b = 0.65\Gamma_{10}$ (solid curves). While the three zero-absorption windows with two of them symmetrically distributing on both sides of the resonant dot still appear in the Im[$n$] curves. The peculiar negative behaviors with zero-absorption of this TQD system interest us most, due to the fact that our proposed scheme is significantly different from the photonic resonant media through the gaseous atomic system, and the zero-absorption property of the left-handed TQD system may be applied to overcome the negative refractive materials with a large amount of absorption. What is more, the manipulation via the external gate voltage and light field is a development technique for all optical communication[37] and optoelectronic devices in the next generation.

In conclusion, the left-handedness with triple zero-absorption windows is demonstrated theoretically in a TQD system. With the typical parameters of a GaAs/AlGaAs heterostructure, the strong responses of simultaneous negative relative electric permittivity and magnetic permeability are observed when the increasing incoherent pumping field and two inter-dot tunnelings among QD1 and QD2, QD2 and QD3 are applied to the TQD system. Then the left-handedness is achieved by the tuned pumping field and two inter-dot tunnelings. What is more, three zero absorption windows emerge in the left-handed frequency bands during the adjustable incoherent pumping field and inter-dot tunnelings coupling the TQD system. The left-handedness with triple transparency windows in the GaAs/AlGaAs heterostructure may overcome not only the challenge in a photonic resonant scheme for left-handedness, but also the main application limitation of the negative refractive materials with a large amount of absorption. The proposed scheme is important due to the fact that the flexible design and several controllable parameters can be easily realized in a multi-dot system. In addition, light controlled by light or by electron tunneling is essential for all optical communication and optoelectronic devices in the next generation.

## References


[1] Veselago V G 1968 *Sov. Phys. Usp.* **10** 509
[2] Feise M W, Bevelacqua P J and Schneider J B 2002 *Phys. Rev.* B **66** 035113
[3] Aydin K, Bulu I and Ozbay E 2007 *Appl. Phys. Lett.* **90** 254102
[4] Pendry J B, Holden A J, Stewart W J and Youngs I 1996 *Phys. Rev. Lett.* **76** 4773
[5] Pendry J B et al 1999 *IEEE Trans. Microwave Theory Tech.* **47** 2075
[6] Shelby R A, Smith D R and Schultz S 2001 *Science* **292** 77
[7] Cubukcu E, Aydin K, Ozbay E, Foteinopoulou S and Soukoulis C M 2003 *Nature* **423** 604
[8] Oktel M Ö, Müstecaplğlu Ö E 2004 *Phys. Rev.* A **70** 053806
[9] Pendry J B 2004 *Science* **306** 1353
[10] Zhao S C, Liu Z D, Zheng J and Li G 2011 *Chin. Phys.* B **20** 067802
Zhao S C, Wu Q X and Gong A L 2013 *Eur. Phys. J.* D **67** 28
[11] He S, Ruan Z C, Chen L and Shen J 2004 *Phys. Rev.* B **70** 115113
[12] Shen J Q, Ruan Z C and He S 2004 *Phys. Lett.* A **330** 487
[13] Zhang H J, Gong S Q, Niu Y P, Li R X and Xu Z Z 2006 *Chin. Phys. Lett.* **23** 1769
Thommen Q and Mandel P 2006 *Phys. Rev. Lett.* **96** 053601
[14] Zhao S C, Liu Z D, Zheng J and Zhang Z Q 2012 *Sci. Chin. Phys. Mech. Astron.* **55** 213
[15] Wu Y and Yang X X 2004 *Phys. Rev.* A **70** 053818
Wu Y and Yang X X 2005 *Phys. Rev.* A **71** 053806
Wu Y and Yang X X 2008 *Physica* E **41** 70
[16] Waugh F R, Berry M J Mar D J, Westervelt R M, Campman K L and Gossard A C 1995 *Phys. Rev. Lett.* **75** 705
[17] Greentree A D, Cole J H, Hamilton A R and Hollenberg L C L 2004 *Phys. Rev.* B **70** 235317
[18] Kloeffel C and Loss D 2013 *Annu. Rev. Condens. Matter Phys.* **4** 51
[19] Gaudreau L, Kam A, Granger G, Studenikin S A, Zawadzki P and Sachrajda A S 2009 *Appl. Phys. Lett.* **95** 193101
[20] Gaudreau L, Granger G, Kam A, Aers G C, Studenikin S A, Sawadzki P, Pioro-Ladriére M, Wasilewski Z R and Sachrajda A S 2011 *Nat. Phys.* **8** 54
[21] Villavicencio J, Maldonado I, Cota E and Platero G 2013 *Phys. Rev.* B **88** 245305
[22] Medford J, Beil J, Taylor J M, Bartlett S D, Doherty A C, Rashba E I, Divincenzo D P, Lu H, Gossard A C and Marcus C M 2013 *Nat. Nanotechnol.* **8** 654
[23] Busl M, Granger G, Gaudreau L, Sánchez R, Kam A, PioroLadriére M, Studenikin S A, Zawadzki P, Wasilewski Z R, Sachrajda A S and G Platero 2013 *Nat. Nanotechnol.* **8** 261
[24] Hsieh C Y, Shim Y P and P Hawrylak 2012 *Phys. Rev.* B **85** 085309
[25] You M H, Li Z G, Gao X, Liu X D, Deng Y, Liu G J, Li L, Wei Z P and Wang X H 2012 *Laser Phys.* **22** 1673
[26] Birkedal D, Leosson K and Hvam J M 2001 *Phys. Rev. Lett.* **87** 227401
[27] Bardeen J 1961 *Appl. Phys. Lett.* **6** 57
[28] Reittu H J 1995 *Am. J. Phys.* **63** 940
[29] Kocharovskaya O, Rostovtsev Y and Scully M O 2001 *Phys. Rev. Lett.* **86** 628
[30] Zhao S C, Zhang S Y and Xu Y Y 2014 *JETP Lett.* **100** 385
[31] Zhao C S and Liu D Z 2009 *Int. J. Quantum Inf.* **7** 747
[32] Zhao C S, Liu D Z and Wu Q X 2010 *Opt. Commun.* **283** 3301
[33] Waugh F R, Berry M J, Mar D J and Westervelt R M 1995 *Phys. Rev. Lett.* **75** 705
[34] Yoo K H, Ram L R Mohan and Nelson D F 1989 *Phys. Rev.* B **39** 12808
[35] Li F L, Fang A P and Wang M 2009 *J. Phys. B: At. Mol. Opt. Phys.* **42** 195505
[36] Mehmannavaz M R and Sattari H 2014 *Laser Phys.* **24** 125201
[37] Borges H S, Sanz L, Villas-Boas J M and Alcalde A M 2013 *Appl. Phys. Lett.* **103** 222101